Simulation of high-resolution x-ray zone plates

Alexei N. Kurokhtin and Alexei V. Popov

Institute of Terrestrial Magnetism, Ionosphere and Radio Wave Propagation, 142190 Troitsk, Moscow Region, Russia

Received November 23, 2000; accepted May 24, 2001; revised manuscript received June 18, 2001

A full-wave approach to quantitative characterization of x-ray zone plate lenses is proposed. Distributed focusing efficiency $\eta(z)$ of a multifocus optical element is defined as the energy flux through the Airy disk of a reference perfect lens with variable focal length z. Maxima of this function characterize diffraction efficiencies and spatial resolution of the zone plate foci. The parabolic wave equation is used to take into account diffraction effects inside the optical element. Rough and fuzzy interface models are introduced to describe realistic zone profiles. Numerical simulation reveals the limited capability of zone width reduction to improve the zone plate imaging performance. The possibilities of second-order focus enhancement by optimization of the zone plate thickness, line-to-space ratio, and zone tilt are studied numerically. © 2002 Optical Society of America

OCIS codes: 050.1960, 050.1970, 340.7460, 000.4430.

1. INTRODUCTION

In this paper our goal is quantitative characterization of the optical performance of state-of-the-art Fresnel microlenses (zone plates) used or designed for x-ray microscopy[1] as a function of zone plate geometry, The zone plate is a diffractive multifocus optical element composed of opaque or semitransparent concentric rings covering alternate Fresnel zones in order to provide constructive interference of the radiation passing through the open zones at the focal point f. The simplest geometrical considerations yield the well-known law for the Fresnel zone radii,

$$r_n = [n\lambda f + (n\lambda/2)^2]^{1/2}, \tag{1}$$

describing a quasi-periodic structure with slowly varying local period

$$d_n = r_{n+1} - r_{n-1} \approx \sqrt{\lambda f/n} (n \gg 1).$$

Here $n = 1, 2, \ldots, N$ is the zone number and λ is the wavelength. In the case of visible-light optics, the zone plate usually can be treated as a plane screen, and the Fresnel–Kirchhoff diffraction theory[2] gives the focal spot radius $\delta \approx 1.22\Delta r$, where $\Delta r = r_N - r_{N-1}$ is the outermost zone width, and allows one to calculate diffraction efficiencies η_m (relative energy flux directed toward different zone plate foci).[1,3] The higher-order foci $m \geqslant 1$ are located at the distances $f_m = f/m$ and can provide better resolution, but usually they are not bright enough. For an idealized opaque, thin Fresnel zone plate, diffraction efficiency to the first order $\eta_1 = 1/\pi^2 \approx 10\%$ of the incident radiation, 50% and 37.5% are the absorbed and scattered radiation, respectively, and the remaining 2.5% are distributed between the higher-order foci.[1,3] Diffraction efficiency into the mth order is $\eta_m = 1/\pi^2 m^2$ for odd numbers m and zero for even orders (for a realistic thick zone plate, the even-order foci may have significant efficiencies).[4,5] In visible-light optics, zone plates are not widely used because of their poor imaging performance compared with that of high-quality lenses. However, in the soft-x-ray spectral range, zone plate microlenses now are the main instrument of imaging and scanning microscopy. For current state-of-the-art Fresnel microlenses in the soft-x-ray range ($\lambda = 0.3$–5 nm), the number of zones can reach 300–1000, the last zone width is ~20–30 nm, numerical aperture NA = 0.04–0.06, and the thickness $b = 50$–500 nm.[6] Prospective zone plates will have greater numerical apertures, and the last zone width $\Delta r \sim 10$ nm, to get closer to the diffraction resolution limit. As such a complication causes considerable manufacturing difficulties, one must be sure that these efforts will give the desired result. Even for the currently used zone plates their characteristics (resolution and efficiency) are usually worse than the common theoretical predictions. Evidently, for future high-performance zone plates, simplified theories may give incorrect (too optimistic) estimates.

In the x-ray spectral band, zone plates are inevitably thick compared with the wavelength, so a full-wave theory is necessary to describe diffraction effects inside the zone plate volume that determine its optical performance. Coupled-wave theory[7,8] and the parabolic equation method[4,5] reveal a complicated redistribution of the transmitted radiation between different diffraction orders. As a result, the plane-screen diffraction theory, even modified to take into account the contribution of the x-ray radiation penetrating through the semitransparent zone material,[9] gives but a qualitative estimate of the focal spot brightness. Although for most of currently used zone plates such a simple theory gives satisfactory results, it cannot explain the drastic drop of efficiency encountered in the attempt to build a high-resolution zone plate with the last zone narrower than 20 nm.[10] Moreover, by its nature it ignores some important effects, such as aberrations, caused by the finite zone plate thickness and unexpectedly high efficiency of the second-order focus. As the focusing efficiency and spatial resolution are crucial parameters for x-ray microscopy, accurate wave theory plays an important role in the development of new high-resolution zone plates.

In this paper some results of numerical simulation are presented. We perform the verification of experimental-

ists' ideas of improving the performance of prospective x-ray zone plates (increasing numerical aperture, the use of second-order focus and zone tilt) in order to understand how justified are the expectations based on qualitative estimates.

2. MATHEMATICAL BASIS

As was stated above, for the accurate simulation of thick inhomogeneous optical elements, one should apply full-wave theory to describe x-ray beam propagation through the element volume. It should be pointed out from the very beginning that simplified scalar one-way wave equations appear to be an adequate approximation for most of the applications in diffractive x-ray optics. The reasons are the small refractivity of all materials in this spectral range and the small numerical apertures of current x-ray microscopes. Mathematically, this means that each component of the electromagnetic field $\mathbf{E}\exp(-i\omega t)$ can be represented as a modulated plane wave $E(x,y,z) = u(x,y,z)\exp(ikz)$ with the slowly varying complex amplitude $u(x,y,z)$. The aforementioned approximations lead to the so-called parabolic wave equation (PWE)

$$2ik\frac{\partial u}{\partial z} + \frac{\partial^2 u}{\partial x^2} + \frac{\partial^2 u}{\partial y^2} + k^2(\epsilon - 1)u = 0, \qquad (2)$$

originally introduced by Leontovich[11] and Fock[12] in the theory of radio propagation, or some of its more accurate versions. Here $k = \omega/c = 2\pi/\lambda$ is the wave number, and $\epsilon = n^2 = (1 - \delta + i\beta)^2$ is complex relative dielectric permittivity, with weak refraction $\delta \ll 1$ and absorption $\beta \ll 1$ in the material taken into account. The parabolic equation method proved to be an efficient analytic and computational tool for a wide variety of high-frequency diffraction problems, including x-ray optics.[4,13] Two advanced approaches to calculate the wave field produced by a realistic x-ray zone plate are used. Actually, both of them are based on the numerical solution of the parabolic wave equation (2).

A. Coupled-Wave Method

The coupled-wave approach considers the zone plate as a graded-period diffraction grating with a slowly varying period. Therefore the solution in such a locally periodic medium is sought as a superposition of local Floquet modes.[7,8] In this way the problem reduces to an infinite system of linear ordinary differential equations for the coupled-mode amplitudes, so the solution of its truncated counterpart can be found by standard numerical algorithms. Usually the second derivatives in the propagation direction are neglected, which makes this approach equivalent to one of the PWE versions. Finally, to obtain an approximate solution of the primary problem, one just has to take into account the slow period variation $d_n \approx \lambda f/r_n$ in accordance with the zone radii law $r_n \approx \sqrt{n\lambda f}$. The output intensity of the mth diffraction order, as a function of radius r, immediately gives the partial diffraction efficiency of the corresponding zone plate segment (local grating contribution into mth focus). The overall zone plate efficiency can be estimated as an integral of these partial efficiencies over the zone plate aperture.[14]

Taking into account zone plate geometry and material, as well as the basic diffraction phenomena in the thick quasi-periodic zone plate structure, the coupled-wave method considerably improves the predictions of diffraction efficiency compared with those of the commonly used plane-screen theory. The truncated system of the coupled-wave equations yields simplified analytic formulas useful for qualitative analysis of the element imaging performance.[14,15] More accurate dependence of diffraction efficiency on the local period and zone plate thickness can be obtained by numerical integration of the full set of coupled-wave equations,[7,8] which opens a way to the design of an optimized zone plate with variable thickness and improved zone positions, different from the traditional Fresnel law Eq. (1). At the same time, this approach has a number of limitations concerning its accuracy and applicability:

- Transition from the model periodic diffraction grating to a graded-period zone plate involves an additional approximation.
- It is difficult to apply the method to describe realistic nonrectangular zone profiles.
- Generally, because of unaccounted-for phase relations, integrated partial efficiencies give too-optimistic an estimate of the overall zone plate diffraction efficiency.

B. Finite-Difference Partial-Wave-Equation Solution inside Optical Elements

It follows from the above considerations that the coupled-wave theory gives a good but not quite exact estimate of the overall zone plate diffraction efficiency. In order to get ultimate quantitative characteristics of the zone plate's imaging performance, it is desirable to apply a straightforward numerical approach that gives the global field distribution throughout the optical system. An efficient computational method, avoiding the approximate substitution of the zone plate with a locally periodic diffraction grating, is the direct numerical solution of the PWE (2) describing one-way narrow-angle propagation in weakly nonuniform media.[4] Being independent of specific assumptions about the element structure, it allows the simulation of more realistic or more sophisticated zone plates not described by the regular rectangular zone model.

Numerical solution of the standard Leontovich parabolic wave equation (2) and its wide-angle modifications has been thoroughly studied.[13] As shown in Ref. 4, for the case of axial symmetry the most adequate is the Crank–Nicholson six-point implicit finite-difference scheme,

$$2ik\frac{u_m^{n+1} - u_m^n}{\tau} + \frac{u_{m+1}^{n+1} - 2u_m^{n+1} + u_{m-1}^{n+1} + u_{m+1}^n - 2u_m^n + u_{m-1}^n}{2h^2} + \frac{u_{m+1}^{n+1} - u_{m-1}^{n+1} + u_{m+1}^n - u_{m-1}^n}{4mh^2} + k^2(\epsilon_m^{n+1/2} - 1)\times\frac{u_m^{n+1} + u_m^n}{2} = 0, \qquad (3)$$

reducing the PWE to a three-diagonal set of linear algebraic equations. Here, τ and h are the mesh steps in the z and r directions, and $u_m^n \approx u(n\tau, mh)$. The linear equations (3), written for $m = 0,1,\ldots,M = A/h$, along with the appropriate boundary conditions, form a consistent set of equations that can be solved step by step, from n to $n + 1$, by the marching method.[16] Note that the three-diagonal character of the transition matrix reduces the computational time considerably compared with the direct matrix inversion.

The approximation error of the finite-difference equations (3) has an order of magnitude $O(h^2 + \tau^2)$. Physically, it is evident that the mesh steps h and τ must be small compared with the transversal and longitudinal scales of the optical element: $h \ll \Delta r$, $\tau \ll b$. More sophisticated numerical error analysis, including wavefront correction and perfectly absorbing (transparent) boundary conditions,[5] allows one to ensure high accuracy in a large computational domain, up to the image plane.

C. Modeling Realistic Zone Profiles

When simulating realistic zone plates, one should take into account miscellaneous manufacturing errors inevitably leading to some, maybe considerable, deterioration of the imaging performance. Among these errors, deformation of annular zones, nonrectangular zone profiles, and stochastic positioning errors are usually mentioned.[3] Another type of manufacturing error—nanometer-scale roughness and fuzziness of the interfaces due to the grainy structure of the zone material and interdiffusion—usually remains beyond the simulation model. Contrary to analytical approaches, numerical solution of the parabolic wave equation can easily cope with these effects. A model example illustrating the influence of the zone interface roughness on the zone plate output field is given in Fig. 1. In Fig. 1(a) the intensity distribution over one period of an idealized zone plate with sharp rectangular zone profile is shown. The specific field pattern caused by edge diffraction and total external reflection[15] is clearly seen. The interface roughness [Fig. 1(b)] splits the field distribution, which leads to a noticeable modification of the output amplitude and local grating diffraction coefficients (~5% in this example); see Fig. 2. In this illustrative example both rough interfaces are chosen symmetrically. Actually, the zone profiles are rather stochastically independent.

In order to simplify further simulation we replace the true permittivity distribution $\epsilon(r,z)$ near the stochastic boundary $r = r_n + \delta(z)$ with a smooth transition layer $\epsilon_{\text{avg}}(r)$ averaging $\epsilon(r,z)$ along the horizontal lines $r = \text{const}$, $0 < z < b$. As is seen from Figs. 1(c), and 2, such a fuzzy interface model yields an output field pattern very close to its rough counterpart. Moreover, such a transition layer is a physically adequate description of the interdiffusion processes at the interfaces between two different zone materials. In what follows, the interfaces between the neighboring zones are smoothed with a transition function $T(x) = [1 + \exp(-x/a)]^{-1}$, where x is the normal distance from a reference interface and a is a characteristic thickness of the transition layer. This fuzziness parameter can be chosen adequately for different manufacturing processes; for a state-of-the-art zone plate we assume it to be approximately 2 nm $\times$ 4 nm.[6] This model gives a more realistic zone profile with rounded tops reminiscent of the SEM images of realistic x-ray zone plates[6] (see Fig. 3), which must improve the predictions of zone plate focusing efficiency. As will be demonstrated below, such zone-profile fuzziness may considerably affect the optical performance of newly designed high-resolution zone plates.

D. Output-Field Analysis

Although the finite-difference algorithm is capable of calculating the global wave-field distribution throughout the

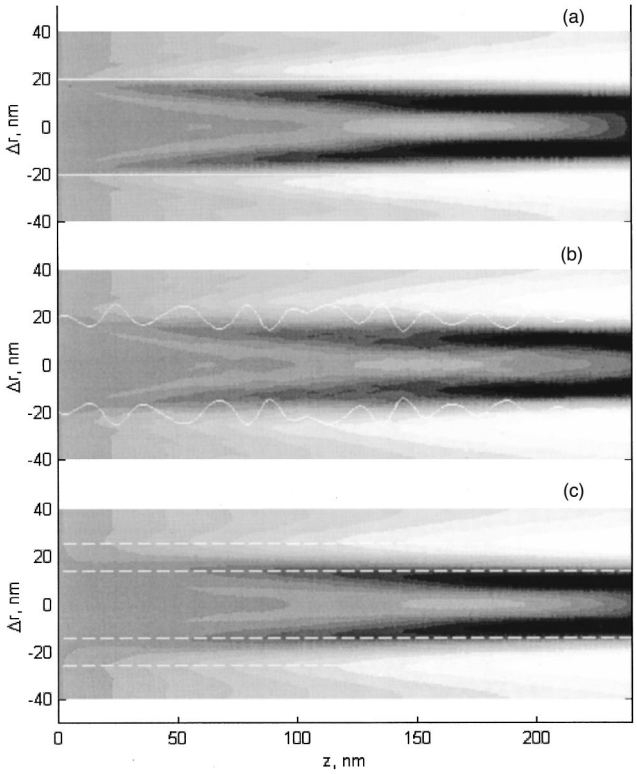

Fig. 1. Intensity distribution over one period of an (a) idealized, (b) realistic rough, and (c) fuzzy zone plate.

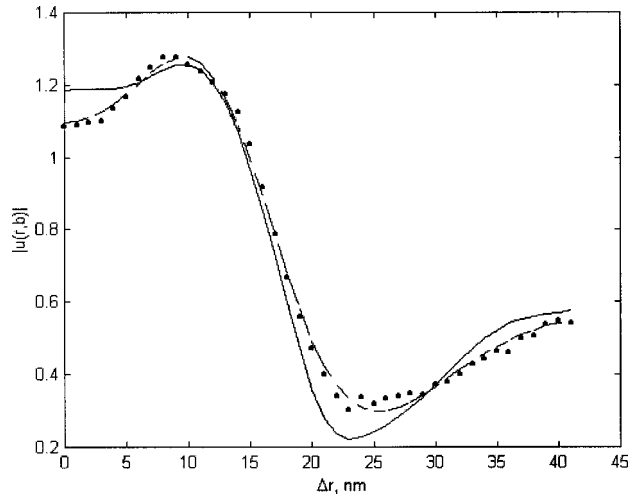

Fig. 2. Half a period fragment of output field amplitude corresponding to Fig. 1 (solid curve, sharp; dots, rough; dashed curve, fuzzy interface).

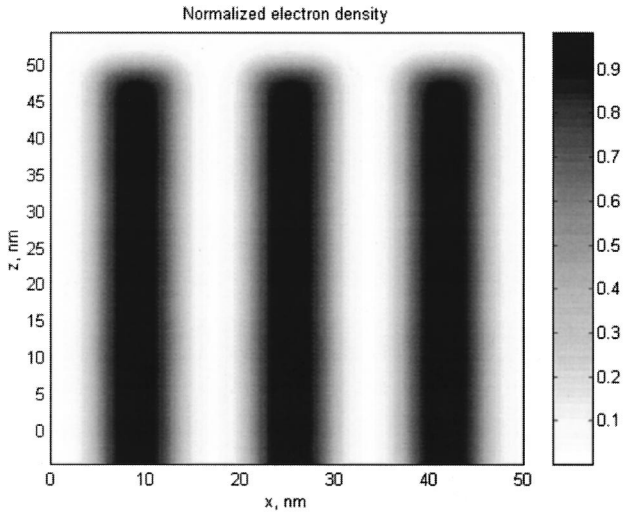

Fig. 3. Segment of fuzzy zone plate profile; fuzzy layer thickness $a = 1$ nm, zone width $\Delta r = 10$ nm.

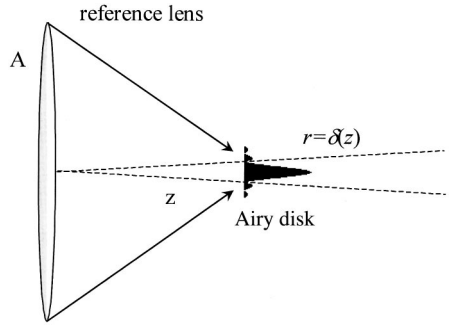

Fig. 4. Airy disk $r = \delta(z) = 3.83z/kA$ of the reference perfect lens used in the definition of DFE.

optical system,[4] for quantitative characterization of zone plate imaging performance it suffices to know the structure of the focal spot. This task can be performed faster and more accurately with a hybrid approach: Kirchhoff integral representation in the focal spot starting from the zone plate output field supplied by the finite-difference PWE solution inside the zone plate body.

To calculate high-NA zone plates or to describe higher-order foci, one has to go beyond the standard narrow-angle PWE [Eq. (2)], keeping the fourth-order phase terms. So, simplifying the general Kirchhoff formula,[2] we obtain an approximate integral representation of the complex wave amplitude,

$$u(r,z) \approx \frac{k}{iz}\exp[ik(r^2/2z)A]\int_0 u_0(\rho)J_0\left(\frac{kr}{z}\rho\right) \times \exp\left[ik\left(\frac{\rho^2}{2z} - \frac{\rho^4}{8z^3}\right)\right]\rho\mathrm{d}\rho, \quad (4)$$

with accuracy sufficient to describe the main and higher-order focal patterns and to take into account spherical aberration arising for higher numerical apertures $NA \sim A/z$ or that is due to the imperfections of the optical element. Here z, r are cylindrical coordinates, and $u_0(\rho)$ is the axially symmetric output field at the current integration point on the back side of the x-ray optical element. This formula can be used for quantitative analysis of any transmission x-ray optical element—in particular, for the estimation of the focal brightness of a realistic x-ray zone plate. First of all, it must be emphasized that the commonly used concept of diffraction efficiency, borrowed from the theory of gratings, does not yield a satisfactory measure of the zone plate focus quality, being unable to take into account how precisely the energy of the corresponding diffraction order is pointed toward the focus. Therefore a more adequate definition of focusing efficiency will be given.

It is well known that a perfect lens of external radius A and focal length f directs ~84% of the overall power πA^2 toward the main bright circle $0 < r < \Delta = \gamma f/kA$ of the Airy pattern emerging in the focal plane $z = f$.[1,2] Here $\gamma \approx 3.83$ is the first zero of the Bessel function $J_1(t)$. This quantity serves as a reference value for diffraction efficiencies of other focusing devices. To characterize the performance of a multifocus optical element, such as a realistic zone plate, we calculate the energy flux passing through an Airy disk of increasing radius $\delta(z) = 3.83z/kA$ as a function of the range variable z and normalize it to the reference value $0.84\pi A^2$ corresponding to the perfect lens; see Fig. 4. This leads to the following definition of the distributed focusing efficiency (DFE) of an arbitrary optical element:

$$\eta(z) = \frac{2.39}{A^2}\int_0^{\delta(z)} |u(r,z)|^2 r\mathrm{d}r. \quad (5)$$

For computational purposes it is convenient to obtain from Eq. (2) the following expression for the longitudinal derivative,

$$\frac{\mathrm{d}\eta}{\mathrm{d}z} \approx 2.39\frac{k\gamma}{A^3z^2}\mathrm{Im}\left\{\int_0^A u_0(\rho)J_1\left(\gamma\frac{\rho}{A}\right) \times \exp\left[ik\left(\frac{\rho^2}{2z} - \frac{\rho^4}{8z^3}\right)\right]\rho^2\mathrm{d}\rho \int_0^A u_0^*(\sigma)J_0\left(\gamma\frac{\sigma}{A}\right) \times \exp\left[-ik\left(\frac{\sigma^2}{2z} - \frac{\sigma^4}{8z^3}\right)\right]\sigma\mathrm{d}\sigma\right\} \quad (6)$$

and then find the DFE $\eta(z)$ by integration.

Formula (5) is quite general and can be used to characterize lenses of utterly different nature and construction (including such singular ones as gravitational lenses[17] forming a continuous focal line instead of the bounded focal spot). For a conventional lens, the initial field amplitude has the form of a single geometrical optics term:

$$u_0(\rho) \approx A(\rho)\exp\{ik[S(\rho) - \rho^2/2f + \rho^4/8f^3]\}, \quad (7)$$

where $S(\rho)$ is the initial wave-front deviation from a perfect sphere. In this case, a single focus appears near the point $z = f$, and formulas (4) and (5) yield an accurate measure of aberration consonant with the classical Strehl brightness definition.[2] In our case of a multifocus Fresnel zone plate, its output field distribution is a two-scale quasi-periodic function,

$$u_0(\rho) = U_0[\rho,t(\rho)] = \sum_{m=-\infty}^{\infty} C_m(\rho)\exp[-imt(\rho)], \quad (8)$$

where the fast variable t is an inverse of Eq. (1):

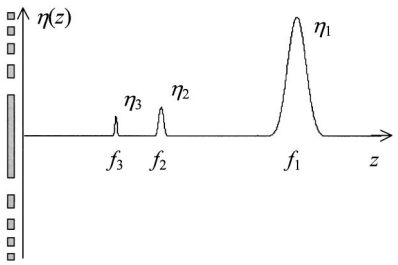

Fig. 5. DFE $\eta(z)$ of a multifocus optical element (zone plate).

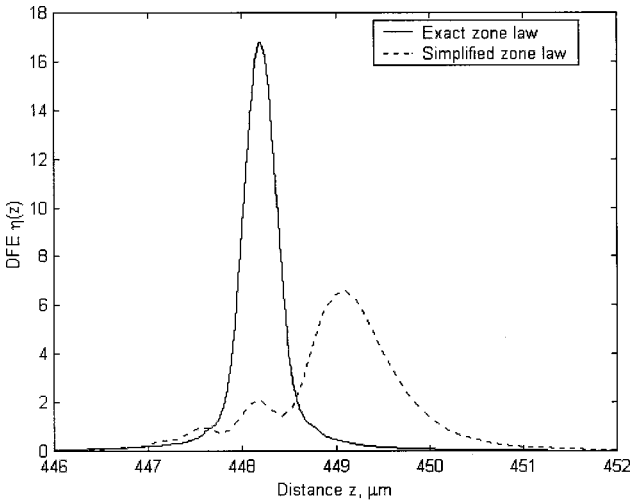

Fig. 6. DFE for two zone plates: solid curve, exact zone law [Eq. (1)]; dashed curve, simplified Fresnel law $r_n = \sqrt{n\lambda f}$.

$$t(\rho) = \pi n = kf(\sqrt{1 + \rho^2/f^2} - l) \approx k(\rho^2/2f - \rho^4/8f^3) \tag{9}$$

and $C_m(\rho) = A_m(\rho)\exp[ikS_m(\rho)]$ are the slowly varying complex amplitudes of the corresponding diffraction orders determined by the local grating parameters. Substituting Fourier series (8) into Eqs. (4) and (5), we obtain an explicit representation of the DFE having sharp maxima near the points $z_m = f/m$, being the positions of different zone plate foci. Their efficiencies are roughly proportional to the integrated partial intensities $A_m^2(\rho)$, whereas the phase shifts $S_m(\rho)$ modify the focal pattern and determine the behavior of $\eta(z)$ near the mth focus, clearly indicating the presence or absence of spherical aberration; see Fig. 5. To give an example, the DFEs of two zone plates with 10-nm outermost zone width and different zone-position laws are plotted in Fig. 6. The dashed curve corresponding to the simplified Fresnel zone law $r_n = \sqrt{n\lambda f}$ shows a rather low, aberrated maximum, whereas the improved zone law [Eq. (1)] gives a perfect bright focus (solid curve).

It must be emphasized that DFE equation (5) is a rectification of the commonly used estimate zone plate diffraction efficiency[3,14] defined as an integral of local energy contributions into the corresponding diffraction order $|C_m(\rho)|^2$ but ignoring phase variations $S_m(\rho)$. In fact, depending not only on the zone plate throughput but also on the accuracy of directing the energy flux to the focal point $z = f$, the value $\eta_m = \eta(f_m)$ gives a true measure of zone plate focusing ability. Of course, the Airy disk of a reference perfect lens is but an *a priori* estimate of zone plate spatial resolution, which may be slightly different. However, this replacement usually does not lead to a noticeable change in the resulting values of the DFE. In dubious cases, the focal pattern $u(r, f)$ can be calculated with Eq. (5) to find the exact value of the lateral resolution δ.

As follows from the above analysis, focal brightness and aberrations of realistic Fresnel zone plates depend in a rather sophisticated manner on the zone position law r_n [by means of the inverse function $t(\rho)$] and the phase of local grating contributions $C_m(\rho)$ to the corresponding diffraction order. Therefore simplified approaches may give misleading (e.g., too-optimistic) results. A full-wave theory is to be used for both the reliable zone plate output field calculation and the accurate analysis of the focal pattern structure.

3. OPTIMIZATION OF ZONE PLATE IMAGING PERFORMANCE

Spatial resolution is one of the crucial parameters of an imaging optical element. It is well known that the lateral resolution of an idealized Fresnel zone plate is set by the width of the outermost zone $d_N \approx \sqrt{\lambda f/N} \approx A/N$, so the main manufacturing efforts are aimed at increasing the number of zones N and refining the zone plate microstructure. At present, the electron-beam writing technique has reached nanometer accuracy, and the prospects of producing zone plates with the outermost zone of ~10 nm are considered. In what follows, some basic limitations imposed by diffraction effects are discussed, and some possible zone plate constructions are quantitatively characterized.

A. Limitation of Improving the Main Zone Plate Focus

Straightforward increase of the zone plate NA seems to be a simple way to improve spatial resolution of the imaging with the first diffraction order. It is believed that increasing the number of zones N, while maintaining the exact Fresnel zone position law, Eq. (1), to compensate for spherical aberration, would reduce the lateral resolution scale δ in accordance with the refinement of the outermost zone Δr. However, our calculations show that the partial diffraction efficiency of the outer zone plate segments decreases drastically starting from a certain radius R_C, which stops further improvement of spatial resolution with enlarging numerical aperture. This effect seems to have a basic cause and can be confirmed analytically by the coupled-wave method, revealing a strong attenuation of the scattering amplitude in the outer part of the zone plate. Roughly speaking, as the outer zones do not contribute energy to the focal spot, the effective numerical aperture and corresponding spatial resolution are limited by the cutoff radius R_C. This effect is even more pronounced for a realistic zone plate with a nonrectangular fuzzy zone profile.

Figure 7 depicts the focusing efficiency to the first order of a family of zone plates with fixed focal length $f = 0.45$ mm for $\lambda = 2.4$ nm and increasing radius A. A typical material, nickel, is chosen for this simulation.

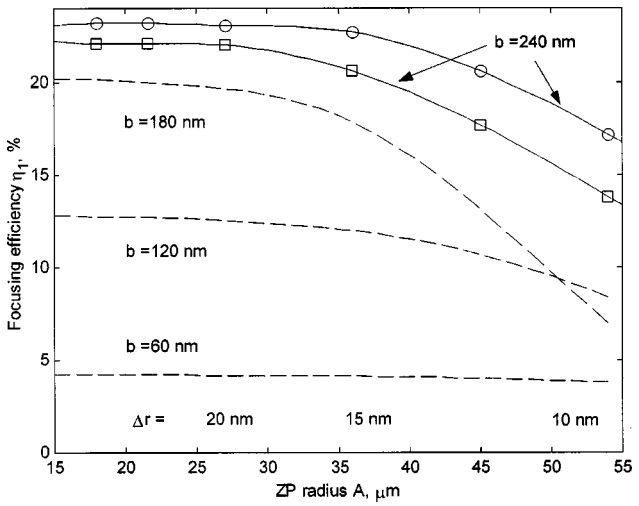

Fig. 7. First-order focusing efficiency as a function of zone plate radius: circles, idealized zone profile; squares, fuzzy profile; dashed curves, efficiency for thinner zone plates.

The starting parameters ($A = 18\,\mu$m, $N = 300$, $f = 0.45$ mm, $\Delta_r = 30$ nm, $b = 240$ nm) are close to those used in the high-resolution x-ray microscope of the Center for X-Ray Optics at Lawrence Berkeley National Laboratory.[18] When the zone plate radius varies from $A = 18\,\mu$m to 65 μm, the number of zones grows more than ten times and the outer zone width reaches the extremely small values $\Delta r \sim 8$ nm accessible with present manufacturing technologies. However, the effect of such technological complication may fall short of the experimentalist's expectations. In fact, even for an idealized zone plate with sharp rectangular zones, the first-order focus efficiency $\eta_1 = \eta_1(A)$ (circles in Fig. 7) decreases by a factor of 2 from 23% for the currently used prototype ($A = 18\,\mu$m, $N = 300$) to 11% for $A = 66\,\mu$m, $N = 4000$. The calculated spatial resolution in the extreme case $\Delta r \sim 8$ nm is ~13 nm instead of the expected value $\delta \approx 1.22\Delta r \approx 10$ nm. For a realistic fuzzy profile with the transition layer thickness $a = 2$ nm (squares in Fig. 7) the outcome is even worse: $\eta_1 = 8.5\%$ for $A = 66\,\mu$m and $\delta = 15$ nm, $\approx 2\Delta r$ which is far from the commonly used estimates. These numerical simulations make doubtful the possibility of achieving a lateral resolution in the main zone plate focus better than $\delta \sim 15$ nm by simply increasing the number of zones.

This crucial drop of diffraction efficiency with decreasing outer zone width is especially pronounced for high-aspect-ratio zone plates when the phase inversion effect at the optimum zone plate thickness of approximately, 200–250 nm is used. For currently used zone plates with lower values of aspect ratio ($b \sim 60$–90 nm), diffraction efficiency predicted both by the full-wave simulation and simplified formulas[9] falls off less rapidly[10]; however, the absolute values $\eta \sim 3$–5% in this case are far from the desired theoretical maximum $\eta_{\max} \sim 25\%$; see dashed curves in Fig. 7.

B. Imaging with Second-Order Focus

Another way to achieve better resolution consists of using higher-order diffraction foci instead of the main one, as spatial resolution should improve as an inverse ratio of the focus number: $\delta_m = \delta_1/m$.[1,3] Still, one should not be very hopeful about high orders, because the expected efficiency η_m drops proportionally to m^{-2} according to the predication of planar Kirchhoff theory. Furthermore, the efficiency must be more sensitive to the imperfections of the zone interfaces as the contributions of the Fresnel subzones lying within one zone plate zone mutually cancel.[1] From these considerations, the second order would be preferable if it were not for its absence for the typical 1:1 line-to-space ratio, according to Kirchhoff theory. But, as full-wave simulation shows, for a realistic thick zone plate the second-order focus is bright enough even for standard zone geometry,[4,5] which motivates further study of the possibilities for its optimization. Thus improved, second-order focus might provide a reasonable balance between spatial resolution and brightness.

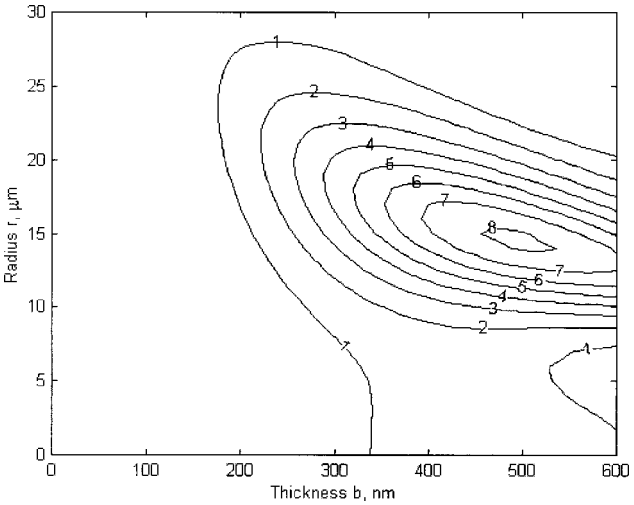

Fig. 8. Partial diffraction efficiency to second order of a nickel zone plate as a function of radius and zone plate thickness for $\lambda = 2.4$ nm, $f_2 = 225\,\mu$m, $L{:}S = 1{:}1$.

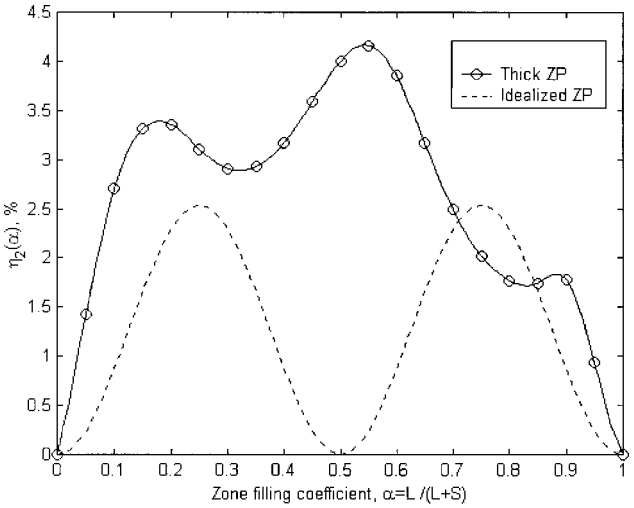

Fig. 9. Second-order focus efficiency η_2 of a nickel zone plate as a function of zone filling coefficient $\alpha = L/d$; $\lambda = 2.4$ nm, $f_2 = 225\,\mu$m, zone plate thickness $b = 480$ nm.

1. Varying Line-to-Space Ratio

As stated above, the second-order diffraction efficiency depends primarily on the line-to-space ratio $L:S$, where L and S are widths of the neighboring opaque and open zones, the local period being $d = L + S$. The plane-screen model[3] predicts that for a standard 1:1 Fresnel zone plate the second order is simply absent while the maximum efficiency $\eta_2 = 1/4\pi^2 \approx 2.5\%$ is achieved for $L:S = 1:3$ or $L:S = 3:1$. For realistic thick zone plates, the relation among diffraction efficiency, line-to-space ratio and thickness is rather complicated. Coupled-wave calculations show that the common 1:1 Fresnel zone plate also can provide a considerable contribution to the second order for a properly chosen thickness. As an example, partial diffraction efficiency as a function of radius r and zone plate thickness b is plotted in Fig. 8 for a $L:S = 1:1$ nickel zone plate of focal length $f_2 = 225\,\mu$m at the soft-x-ray wavelength $\lambda = 2.4$ nm. It can be seen that for any chosen thickness b the function $\eta_2(r)$ is strongly nonuniform with a maximum achieved in a narrow annular segment. The dependence of the second-order focusing efficiency of this zone plate on the zone filling coefficient $\alpha = L/d$ for a fixed thickness $b = 480$ nm is shown in Fig. 9 (solid curve, full-wave calculation; dashed curve, reference thin zone plate). It is clear that the two models have little resemblance in their behavior. According to the full-wave calculations, the optimum efficiency is reached near the common zone plate geometry $\alpha = 0.5$ ($L:S = 1:1$). It gives the maximum value of the partial diffraction efficiency of ~8% for $r \approx 15\,\mu$m and total cumulative second-order focusing efficiency $\eta_2 \approx 4\%$; see Fig. 9. This example shows that there is still room for further optimization by designing zone plates of variable line-to-space ratio and variable thickness. However, numerical experiments show that it seems unlikely to surpass in this way efficiencies of ~6–8%.

To give a realistic example, let us consider a possible prospective zone plate construction for operation in the second diffraction order in the water window spectral region ($\lambda = 2.4$ nm). Its parameters could be as follows: diameter $D = 0.1$ mm, number of zones $N = 1160$, main focus position $f = 0.9$ mm, the smallest period $d_N = 43$ nm. Estimating the achievable minimum feature size as 10 nm, we choose the line-to-space ratio $L:S = 1:3$. Optimized for second-order focus brightness, the constant thickness $b = 220$ nm gives the following imaging characteristics: focusing efficiency $\eta_2 \approx 5\%$, spatial resolution $\delta_2 \approx 13$ nm, which agrees with the Rayleigh criterion $\delta_2 = 1.22d/4\lambda$.

2. Specular Enhancement of Second-Order Focus

As shown in Subsection 3.B.1, without a considerable change in the zone plate construction it is impossible to get diffraction efficiency to the second order exceeding a few percent. Keeping in mind further improvement, let us turn to the promising idea of slanting the opaque zones in order to exploit total external reflection from their skew interfaces.[7] A sketch of such a zone plate with tilted zones is shown in Fig. 10. Recent numerical simulation of tilted gratings by the coupled-wave method shows that it is possible to achieve very large diffraction efficiencies into the higher orders, up to ~60%.[19] The reason for such impressive enhancement is that each illuminated opaque zone interface acts as a mirror reflecting the incident radiation toward the desired order. Positioning of the zones according to the Fresnel law, Eq. (1), should provide the constructive interference of the radiation, reflected from each interface, in the focal spot. One can easily see that the tilt angle between the zone interface and the optical axis should grow with radius r. Consider, for example, a plane-wave focusing into the mth order: Each horizontal ray is to be deflected by the angle $\phi_m(r) = \mathrm{atan}(r/f_m)$, where r is the distance from the optical axis. For small NA, the zone tilt angle $\psi_m(r)$, being half of the deflection angle, is approximately proportional to the radius:

$$\psi_m(r) = \phi_m(r)/2 \approx mr/2f. \tag{10}$$

It is expected that a zone plate with zone tilt law (10) will demonstrate crucial enhancement of the mth focus.

In order to verify this hypothesis for a realistic zone plate model, we performed a series of full-wave simulations. In what follows we study the influence of the zone tilt on the second-order focusing efficiency of the prospective zone plate considered in Subsection 3.B.1. The coupled-wave calculation for this case shows that the local grating efficiency in the outer part of the zone plate reaches values up to 50%, see Fig. 11. Here the contour lines of the partial diffraction efficiency to the second order $\eta_2(r, b)$, being a function of radius and zone plate thickness, are shown. To calculate the cumulative second-order focusing efficiency we use the combined technique described in Subsections 2.B and 2.D: finite-difference PWE (1) solution inside the zone plate volume, and energy-flow calculation (5) via Kirchhoff integration (4). For the thickness $b = 850$ nm, which is optimal for the outer part of the zone plate, the second-order focusing efficiency sums up to 22%, which, although not so striking compared with the prediction of the coupled-wave grating theory,[19] still exceeds all known experimental results for higher-order foci and is comparable with the typical first-order efficiencies of the best soft-x-ray zone plate.[6]

Although it is apparently worth trying to fabricate such blazed zone plates, this approach has not been carried out so far because of the difficulties in the implementation of reactive ion etching for producing deep, slanted interzone grooves. Another way to achieve similar performance may consist in bending an ordinary thick zone plate slightly as a whole in such a way that it would take on a spherical shape with the center at the double focal length of the corresponding order (second in our case); see Fig. 12. It can be easily seen that for small NA the relation [relation (10)] between the zone tilt angle and radius will be approximately satisfied. For the example considered, the maximum tilt angle is approximately $\beta = A/f \approx 3.2°$, which seems to be achievable by modern manufacturing technologies.

3. Optimal Thickness of Tilted Zone Plates

The discrepancy between very optimistic predictions of grating theory and more moderate results of the full-wave zone plate simulation has a simple explanation: Not only the zone tilt angle but also the optimum thickness depends on the local grating period.[19] Therefore not all

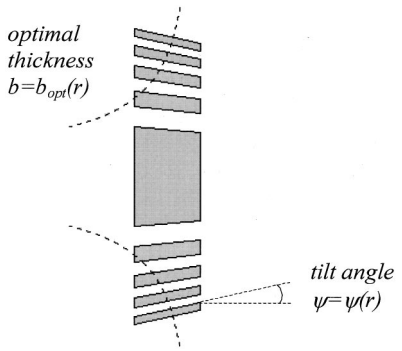

Fig. 10. Sketch of a tilted zone plate: $\psi = \psi(r)$ is variable tilt angle; dashed curves show optimal thickness $b(r)$.

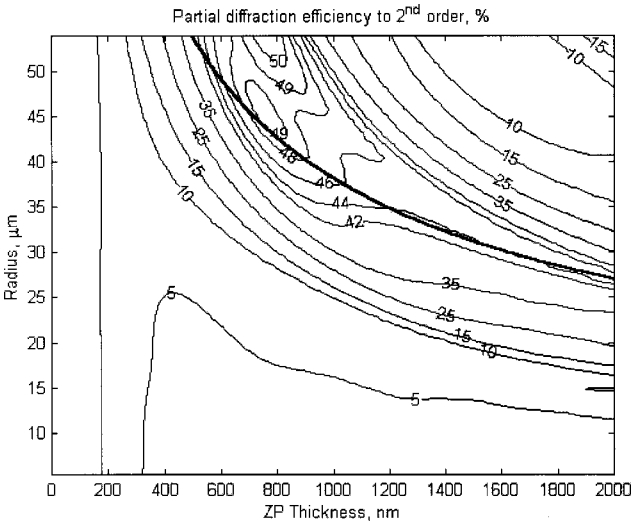

Fig. 11. Local grating efficiency to the second order (coupled-wave calculation). The bold curve shows the optimum geometrical thickness.

segments of the zone plate with constant thickness show optimal performance, which is confirmed by local Fourier analysis of the output wave field. For the purpose of further improvement, it is useful to estimate the optimum thickness of a tilted zone plate from simple geometrical considerations. Roughly, in this case each incident ray entering the open zone should undergo a single reflection from the tilted opaque zone interface and leave the zone plate volume unobstructed, contributing to the desired diffraction order; see Fig. 13. Such geometry, eliminating reflections from the opposite opaque zone that would redirect a part of beam energy toward the undiffracted zero order, determines the proper thickness b_{opt} as a function of local period and tilt angle. For the case of a plane wave incident along the optical axis, the optimal thickness found from Fig. 13 is $b_{\mathrm{opt}} \approx S/\psi$, where S is the open zone width (space) and ψ is the zone tilt angle. If ψ is chosen to enhance the reflection into mth order, $\psi = \psi_m \approx (m\lambda)/(2d)$, then the proper thickness is

$$b_{\mathrm{opt}}(r) \approx \frac{2\lambda f^2}{(1 + L/S)mr^2}. \tag{11}$$

Despite the unaccounted-for small diffraction effects, this simple formula (Fig. 11, bold curve) is in a good agreement with the optimum thickness found from coupled-wave calculations (the ridge of the grating efficiency relief shown by the contour lines in Fig. 11).

These geometrical considerations clarify the role of the line-to-space ratio for tilted zone plate construction. Neglecting diffraction effects and radiation penetrating through the opaque zones, one can estimate the local grating efficiency roughly as S/d, which tends to 100% with diminishing width of the opaque zone $L/S \to 0$. Reaching this optimum is limited by apparent technological constraints, and, further, the laws of reflection become more complicated when the material layer thickness L is comparable with the penetration depth $\Lambda \sim [k(\psi_{\mathrm{total}}^2 - \psi^2)^{1/2}]^{-1}$ [here, $\psi_{\mathrm{total}} = (1 - \mathrm{Re}\,\epsilon)^{1/2}$ is the angle of total external reflection; for the outer zones in our zone plate example, Λ is ~5 nm, which means that the geometrical reflection model here may have only qualitative character].

Another technological difficulty revealed by the geometrical formula (11) is the very high value of the optimum zone plate thickness in its central part (see Fig. 10), which would lead to practically unachievable aspect ratios (thickness to period, $b{:}d$). However, this part of the zone plate, giving small contribution to the focus and being blocked in most optical schemes, is of little importance.[1,3] For larger radii, the optimum thickness $b_{\mathrm{opt}}(r)$ has the reasonable order of magnitude $b \sim 1\ \mu$m.

Consider now the zone plate of Subsection 3.B.2 to see how its performance could be improved by means of thickness variation. Let us confine ourselves to aspect ratios of ~20, which gives maximum thickness $b_0 = 2\ \mu$m for the inner zones. Starting from the radius $R_0 = f[S\lambda/(L + S)b_0]^{1/2} \approx 27\ \mu$m, the zone plate thickness

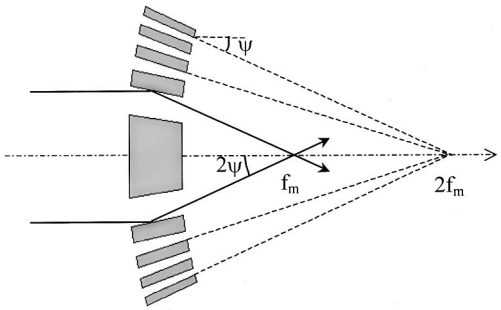

Fig. 12. Sketch of a bent zone plate.

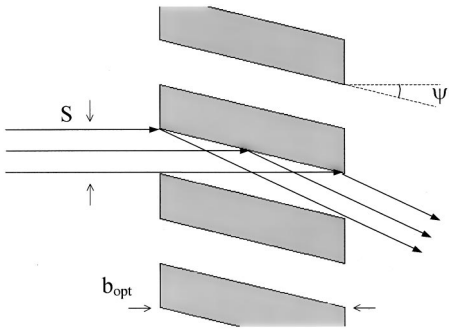

Fig. 13. Geometrical illustration of the optimal thickness for a tilted zone plate.

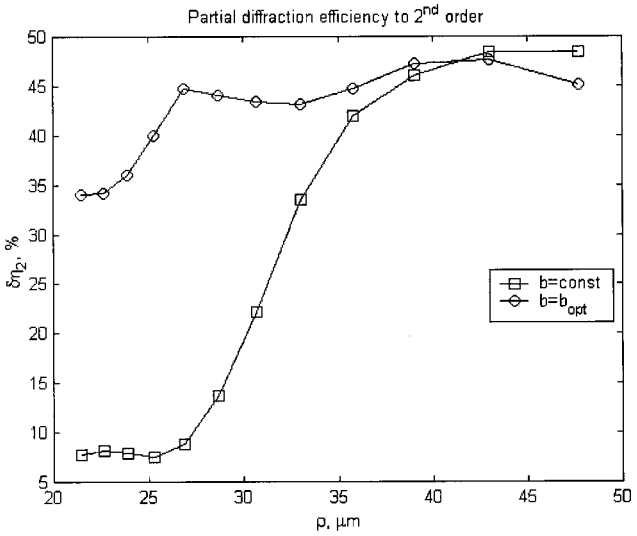

Fig. 14. Partial diffraction efficiencies obtained from the zone plate output-field analysis for a constant-thickness zone plate (squares) and its optimized variable-thickness modification (circles).

Table 1. Dependence of Second-Order Focusing Efficiency η_2 on Fuzzy Layer Thickness a for a Constant Thickness Zone Plate and Its Variable-Thickness Modification

	a (nm)				
η_2 (%)	0	1	2	3	4
$b = 850$ nm	22.0	21.4	19.2	16.5	13.7
$b = b_{\text{opt}}$	32.0	30.0	25.8	22.3	16.9

decreases to its minimum value $b(A)$ in accordance with the geometrical formula (11):

$$b = b_0, \qquad r < R_0,$$
$$b = b_0(R_0/r)^2, \qquad r > R_0. \tag{12}$$

From the numerical simulation it follows that such change of zone plate construction would increase its focusing efficiency η_2 to 32%. This is due to the more uniform distribution of the partial diffraction efficiency along the zone plate radius, and hence a larger part of the zone plate makes a considerable contribution to the focal spot. Figure 14 depicts the radial distribution of the local grating efficiency for this variable-thickness zone plate (circles) in comparison with its constant-thickness prototype of Subsection 3.B.2 (squares). Numerical experiments show that this value of focusing efficiency into the second order (~30%) is close to the absolute maximum accessible within the chosen technological constraints (thickness, aspect ratio, line width, etc.).

4. Influence of Manufacturing Errors

An important question remains: How sensitive will the imaging performance of such atypical zone plates be to manufacturing errors, such as the imperfections of the zone interfaces? We can account for the interface roughness with the fuzzy-zone model of Subsection 2.C.

Table 1 illustrates the dependence of the blazing effect on the interface quality for two tilted zone microlenses of Subsections 3.B.2 and 3.B.3. One can see that in both examples the focusing efficiency into the second-order η_2, as a function of the fuzzy-layer thickness a, drops by a factor of 1.5 to 2 when turning from an idealized perfectly smooth interface to a more realistic value $a = 4$ nm. Moreover, the optimized zone plate with $b = b_{\text{opt}}(r)$ will appreciably surpass its constant-thickness counterpart $b = 850$ nm only if a good interface quality of approximately $a = 2$ nm is maintained.

4. CONCLUSION

In this paper an accurate and efficient simulation technique has been developed for quantitative characterization of the focusing ability of a diffraction-limited multifocus optical element. This method was applied to studying the imaging performance of prospective soft-x-ray zone plate lenses. Numerical simulation has demonstrated that spatial resolution better than 15 nm is hardly achievable by simply increasing the number of zones because of the basic diffraction effects that limit the first-order focus brightness. It turns out that the focusing efficiency drops to values less than 10% with decreasing zone width. This effect depends crucially on the interface roughness, which can be described with a fuzzy-zone model.

The second-order focus may show better performance provided that zone plate thickness and line-to-space ratio are optimized. The effect of specular reflection from the tilted zone interfaces could be used for increasing the second-order focus efficiency up to approximately 25–30% if the manufacturing complications (large aspect ratio, variable zone plate thickness, and appropriate variable zone tilt) were overcome.

ACKNOWLEDGMENT

We are grateful to A. V. Vinogradov, Yu. V. Kopylov, D. T. Attwood, and E. H. Andersson for their interest in this work and fruitful discussions. This work was supported in part by Lawrence Berkeley National Laboratory under subcontract No. 6496135.

A. Kurokhtin's e-mail address is kur@izmiran.rssi.ru.

REFERENCES

1. D. T. Attwood, *Soft X-Rays and Extreme Ultraviolet Radiation, Principles and Applications* (Cambridge U. Press, Cambridge, N.Y., 1999).
2. M. Born and E. Wolf, *Principles of Optics* (Pergamon, Oxford, UK, 1980).
3. A. G. Michette, *Optical Systems for Soft X-Rays* (Plenum, New York, 1986).
4. Yu. V. Kopylov, A. V. Popov, and A. V. Vinogradov, "Application of the parabolic wave equation to x-ray diffraction optics," Opt. Commun. **118**, 619–636 (1995).
5. A. V. Vinogradov, A. V. Popov, Yu. V. Kopylov, and A. N. Kurokhtin, *Numerical Simulation of X-Ray Diffractive Optics* (A&B Publishing House, Moscow, 1999).
6. *X-Ray Microscopy*, Proceedings of the 6th International Conference (American Institute of Physics, Melville, N.Y., 2000).

7. J. Maser and G. Schmahl, "Coupled wave description of the diffraction by zone plates with high aspect ratios," Opt. Commun. **89**, 355–362 (1992).
8. G. Schneider, "Zone plates with high efficiency in high orders of diffraction described by dynamical theory," Appl. Phys. Lett. **71**, 2242–2244 (1997).
9. J. Kirz, "Phase zone plates for x-ray and the extreme UV," J. Opt. Soc. Am. **64**, 301–309 (1974).
10. D. Tennant, S. Spector. A. Stein, and C. Jacobsen, "Electron beam lithography of Fresnel zone plates using a rectilinear machine and trilayer resists," in *X-Ray Microscopy*, Proceedings of the 6th International Conference (American Institute of Physics, Melville, N.Y., 2000), pp. 601–604.
11. M. A. Leontovich, " A method to solve problems of electromagnetic wave propagation along the earth's surface" (in Russian), Izv. Akad. Nauk USSR Ser. Fiz. **8**(1), 16–22 (1944).
12. V. A. Fock, *Electromagnetic Diffraction and Propagation Problems* (Pergamon, Oxford, UK, 1965).
13. M. Levy, *Parabolic Equation Method for Electromagnetic Wave Propagation* (Institute of Electrical Engineers, London, 2000).
14. V. E. Levashov and A. V. Vinogradov, "Analytical theory of the zone plates efficiency," Phys. Rev. E **49**, 5797–5803 (1994).
15. Yu. V. Kopylov, A. V. Popov, and A. V. Vinogradov, "Diffraction phenomena inside thick Fresnel zone plates," Radio Sci. **31**, 1815–1822 (1996).
16. R. D. Richtmayer and K. W. Morton, *Difference Methods for Initial Value Problems*, 2nd ed. (Interscience, New York, 1967).
17. P. V. Bliokh and A. A. Minakov, "Diffraction of light and lens effect of the stellar gravitational field," Astrophys. Space Sci. **34**, L7–L9 (1975).
18. W. Meyer-lise, G. Denbeaux, L. E. Johnson, W. Bates, A. Lucero, and E. H. Anderson, "The high resolution x-ray microscope XM-1," in *X-Ray Microscopy*, Proceedings of the 6th International Conference (American Institute of Physics, Melville, N.Y., 2000), pp. 129–134.
19. G. Schneider and J. Maser, "Zone plates as imaging optics in high diffraction orders described by coupled wave theory," in *X-Ray Microscopy and Spectromicroscopy*, Proceedings of the 5th International Conference on X-Ray Microscopy and Spectromicroscopy, (Springer-Verlag, Berlin, 1998), pp. IV-71–IV-76 (on CD).